ELSEVIER

Journal of Photochemistry and Photobiology A: Chemistry 143 (2001) 99–108

Journal of Photochemistry and Photobiology A:Chemistry

www.elsevier.com/locate/jphotochem

Photochemistry of the $[Fe(CN)_5N(O)SR]^{3-}$ complex A mechanistic study

Konrad Szaciłowski [a], Janusz Oszajca [a], Andrea Barbieri [b], Andrzej Karocki [a], Zbigniew Sojka [a], Silvana Sostero [b], Rita Boaretto [b], Zofia Stasicka [a,*]

[a] *Faculty of Chemistry, Jagiellonian University, Ingardena 3, 30-060 Kraków, Poland*
[b] *Department of Chemistry, University of Ferrara, Via Borsari 46, 44100 Ferrara, Italy*

Received 20 March 2001; received in revised form 21 June 2001; accepted 27 June 2001

Abstract

Photochemical behaviour of the title complex ($RS^- =$ mercaptosuccinate) was defined as photodissociation and photooxidation–substitution reactions induced by the MLCT transition. The stable products as well as shortly lived intermediate species were identified and characterised by ESR and fast UV/VIS spectroscopic methods. The photodissociation of excited $[Fe(CN)_5N(O)SR)]^{3-}$ (Scheme 1, path a) shifts the equilibrium between the complex and $[Fe(CN)_5NO]^{2-}$ (Eq. (1)). Photooxidation–substitution reaction (Scheme 1, path b) leads to formation of the $[Fe^{III}(CN)_5SR]^{3-}$ complex and the $RSNO^{\bullet -}$ radical. The radical generates different NO-donors in secondary thermal processes, which, however, have no noticeable influence on the nitrosation capacity of the system. Moreover, due to the fast reactions in equilibrium between nitroprusside and its thiolate derivative (Eq. (1)), the photooxidation–substitution is really a photocatalytic process and the nitrosation agents are produced mostly at the expense of nitroprusside, whereas the $[Fe(CN)_5N(O)SR]^{3-}$ complex behaves as a photocatalyst. Its photoreactivity induced by visible light ($\lambda_{max} = 526$ nm, $\varepsilon_{max} = 6000$) reduces the threshold energy of the process to nearly the phototherapeutic window.

Keywords: Photodissociation; Photooxidation–substitution; Photocatalysis; Nitroprusside; Mercaptosuccinate; *S*-nitrosothiol

1. Introduction

Recent developments in phototherapy revealed that the NO delivery to selected tissues is of great practical importance [1]. This stimulates search for compounds able to generate NO or reactive NO-donors using low-energy irradiation. The interest is focussed especially on *S*-nitrosothiols and metal nitrosyl complexes. Several systems, including different metal nitrosyls such as $[Fe(CN)_5NO]^{2-}$ [1,2], red and black Roussin's salts ($[Fe_2S_2(NO)_4]^{2-}$ and $[Fe_3S_4(NO)_7]^{-}$) [1–6], ruthenium (e.g. [Ru(tpp)(NO)(ONO)]) [1] and chromium complexes (e.g. $[Cr(cyclam)(NO_2)_2]$) [7,8], have recently been studied. All the investigated systems were found to release nitric oxide upon visible irradiation, but low absorbance and low quantum yield of the NO photorelease within the phototherapeutic window made the systems not very useful for the therapeutic applications. Also different *S*-nitrosothiols, RSNO, have been studied as potential NO-photodonors [9]. They have been suggested to be effective against leukemic cells due to NO and $RS^{\bullet}$ generation [10]. Some new aspects of thermal behaviour of the $[Fe(CN)_5N(O)SR]^{3-}$ complexes and their photoreactivity reported recently [11] stimulated us to study in more detail these medically relevant complexes. Sodium nitroprusside (NP) itself is a widely used nitrovasodilator, but detailed mechanism of its physiological action is still not fully understood. It is supposed, however, that its interaction with thiolate groups of aminoacids and peptides plays crucial role in the metabolism of nitroprusside [12]. It is known from the previous studies [5,11–20] that nitroprusside and thiolates generate *S*-nitrosothiol complexes in the reversible reaction (1).

$$[Fe(CN)_5NO]^{2-} + RS^- \rightleftarrows [Fe(CN)_5N(O)SR]^{3-} \quad (1)$$

In most cases, the reaction product is thermally unstable and in redox decomposition yields Fe(I) complex and disulphide (2–3) [5,10,11,14–20].

$$[Fe(CN)_5N(O)SR]^{3-} \rightarrow [Fe(CN)_5NO]^{3-} + \tfrac{1}{2}RSSR \quad (2)$$

$$[Fe(CN)_5N(O)SR]^{3-} + RS^- \rightarrow [Fe(CN)_5NO]^{3-} + RSSR^{\bullet -} \quad (3)$$

* Corresponding author. Fax: +48-12-633-5392.
E-mail address: stasicka@chemia.uj.edu.pl (Z. Stasicka).

1010-6030/01/$ – see front matter
PII: S1010-6030(01)00519-6

Insertion of an electronegative substituent into the thiol moiety increases, however, thermal stability of the $[Fe(CN)_5N(O)SR]^{3-}$ complex [19]. Recently, it was found that the complex with $RS^- =$ mercaptosuccinate is thermally stable and undergoes photooxidation–substitution reaction like its parent complex [11].

Photochemistry of nitroprusside is well documented. Exposure to high-energy radiation ($\lambda \leq 313$ nm) induces photoreduction (4) [21–23]

$$[Fe(CN)_5NO]^{2-} + solv \xrightarrow{h\nu} [Fe(CN)_5NO]^{3-} + solv^{\bullet +} \quad (4)$$

whereas irradiation with light of lower energy ($\lambda > 313$ nm) causes photooxidation–substitution reaction (5) [21–27].

$$[Fe(CN)_5NO]^{2-} + OH^- \xrightarrow{h\nu} [Fe(CN)_5OH]^{3-} + NO^{\bullet} \quad (5)$$

Quantum yield of the process (5) decreases with increase in irradiation wavelength and increasing pH. In low-energy region quantum yield of the photooxidation–substitution is very low ($\Phi_{546} = 0.006 \pm 0.001$) [11], which makes the system not very useful for the NO photodelivery.

The $[Fe(CN)_5N(O)SR]^{3-}$ photosensivity is bathochromically shifted in relation to that of nitroprusside, and its absorption within the low energy range is relatively high ($\varepsilon_{526} = 6100 \pm 100\,M^{-1}\,cm^{-1}$). The photoreaction produces nitrosothiyl radical anions and relatively stable $[Fe(CN)_5SR]^{3-}$ complex, with quantum yield equal to 0.022 ± 0.002 at 578 nm [11]. These characteristics of the nitroprusside–thiolate system fit well to the expected photomedical applications. This stimulated us to investigate the mechanism and products of the photolysis in more detail.

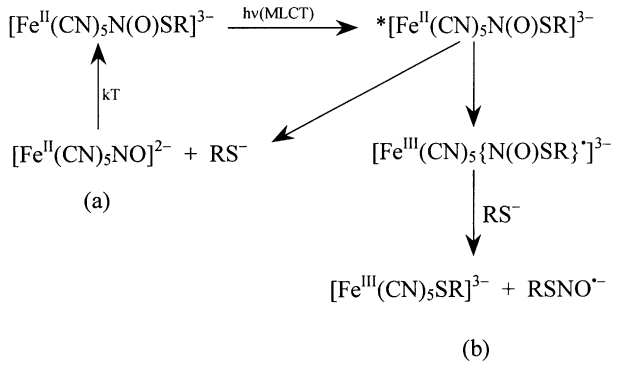

Scheme 1.

2. Results and discussion

2.1. Primary processes

To study primary photochemical processes, the solution containing nitroprusside, mercaptosuccinate and $[Fe(CN)_5N(O)SR]^{3-}$ in equilibrium (Eq. (1)) was photolysed with a laser pulse at $\lambda = 532$ nm. The radiation, absorbed only by the $[Fe(CN)_5N(O)SR]^{3-}$ complex, caused immediate decrease in the substrate absorption recorded at 520 nm (Fig. 1a), which was followed by an appearance of two transient species absorbing within 300–380 nm (Fig. 2) and by increase in absorption at ~700 nm, due to formation of a relatively stable product (Fig. 1).

The stable product, characterised by an intensive absorption within the visible range ($\lambda_{max} = 700$ nm, $\varepsilon = 2700\,M^{-1}\,cm^{-1}$) and half-life equal to 650 s, has been identified earlier as the $[Fe^{III}(CN)_5SR]^{3-}$ complex [11].

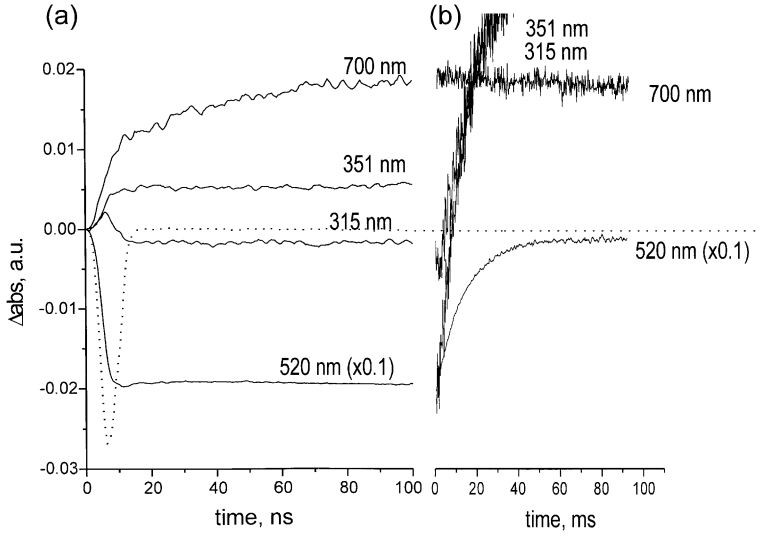

Fig. 1. Kinetic traces following a 532 nm laser photolysis of 2.90×10^{-4} M $[Fe(CN)_5N(O)SR]^{3-}$ in equilibrium with 1.71×10^{-3} M nitroprusside and 9.71×10^{-3} M RS^- (RS^- = mercaptosuccinate) at pH = 10; (a) traces recorded within first 100 ns upon pulse characteristic of: $[Fe(CN)_5N(O)SR]^{3-}$ (520 nm, scaled down 10 times), transient species (315 and 351 nm) and stable product (700 nm); (b) traces recorded within 100 ms; the sharp minimum within 0–15 ns represents laser pulse duration.

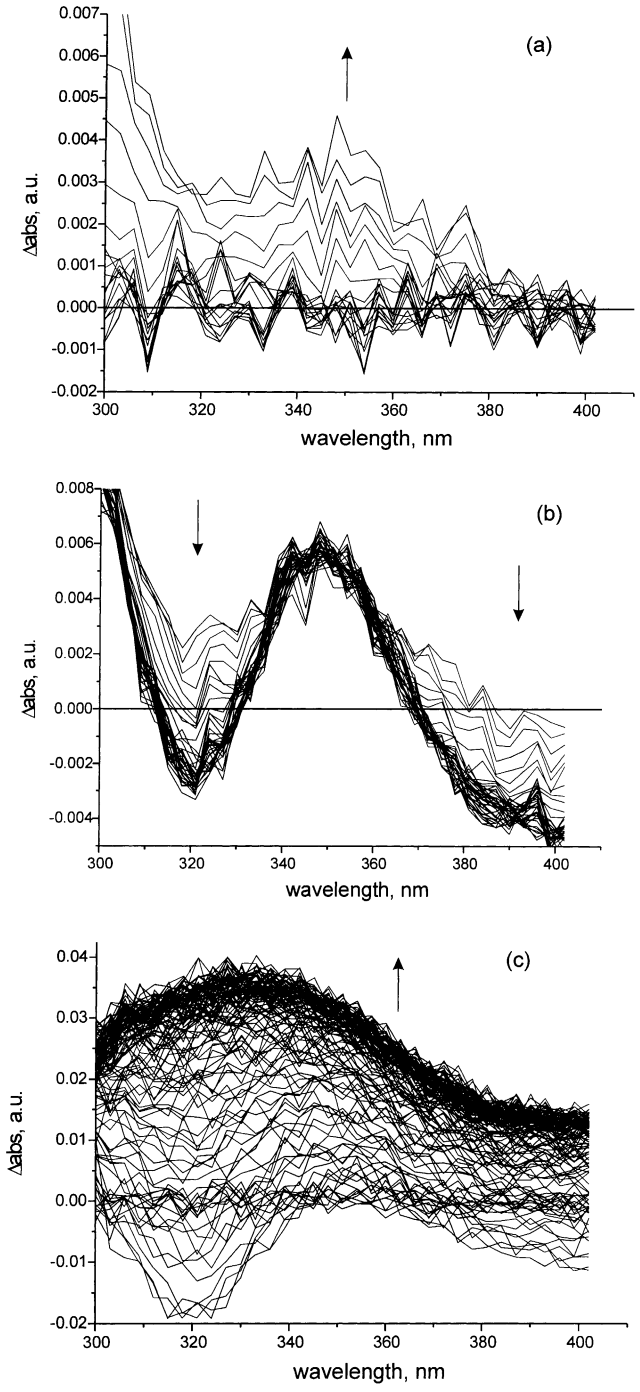

Fig. 2. Transient spectra of solution containing 2.9×10^{-4} M $[Fe(CN)_5N(O)SR]^{3-}$ in equilibrium with 1.71×10^{-3} M nitroprusside and 9.71×10^{-3} M RS^- (RS^- = mercaptosuccinate) at pH = 10; (a) recorded within first 5 ns upon 532 nm laser photolysis; (b) within 5–30 ns; and (c) within 1–100 ms.

Its formation was found, moreover, to be accompanied by growing of a broad, distinctly anisotropic, ESR signal with $g_\perp = 2.126$ and $g_\parallel = 2.086$ at 77 K and $g_{iso} = 2.086$ at room temperature (Fig. 3, Table 1). The parameters of the signal resemble well those of the similar low spin Fe(III) complexes containing both cyano and thiolato ligands [28].

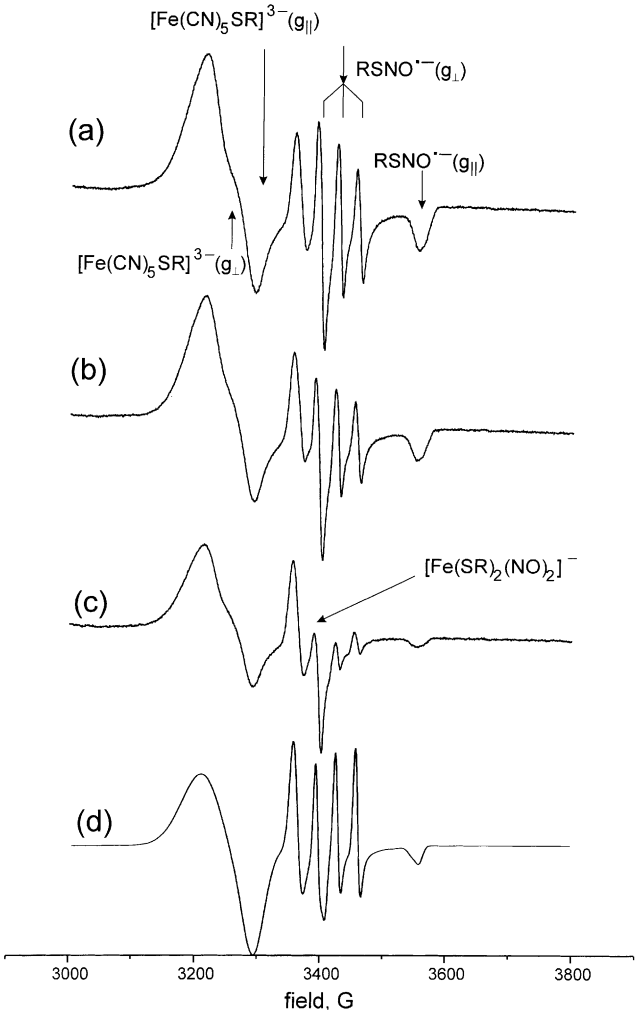

Fig. 3. (a) ESR spectra of irradiated ($\lambda_{irr} \geq 380$ nm) solutions of $[Fe(CN)_5N(O)SR]^{3-}$ generated from 5×10^{-3} M $[Fe(CN)_5NO]^{2-}$ and 0.015 M RS^- (RS^- = mercaptosuccinate) in water–glycol glass at 77 K; (b) after partial and (c) almost complete annealing. Line (d) depicts the simulation of the first spectrum.

Transformation of the $[Fe^{II}(CN)_5N(O)SR]^{3-}$ complex into the $[Fe^{III}(CN)_5SR]^{3-}$ ion had to include both charge-transfer and substitution steps. The 532 nm excitation results in the MLCT transition towards the RSNO ligand [5,11,19]. The charge transfer is effective in population of the antibonding orbital localised at the RSNO ligand [29] and, in consequence, in cleavage of the N–S bond generating $[Fe(CN)_5NO]^{2-}$ and thiolate anion (Scheme 1, path a). The effective electron transfer outside the Fe-centre may as well lead to formation of the Fe(III) complex and the $RSNO^{\bullet-}$ radical, easily substituted by the RS^- ligand (Scheme 1, path b).

The dissociation reaction (Scheme 1, path a) could be observed only indirectly. It was signalled by the laser induced decrease in the $[Fe(CN)_5N(O)SR]^{3-}$ concentration, which was significantly larger than the increase in concentration of $[Fe^{III}(CN)_5SR]^{3-}$. On the average, only about 30% of the

Table 1
Spectral characteristics of substrates and products of photochemical reaction in the system $[Fe(CN)_5NO]^{2-}$-mercaptosuccinate

Species	UV/VIS, (λ_{max}, nm; ε, $M^{-1}\,cm^{-1}$)	ESR parameters: g and A (^{14}N) (G), A (^{1}H) (G) tensors	Reference
$[Fe(CN)_5NO]^{2-}$	264 (900) 330 (40) 393 (25) 497 (8)	Diamagnetic	[33]
$[Fe(CN)_5NO]^{3-}$	345 (3500) 430 (550)		[34]
		$g_\perp = 2.005$, $^{N}A_\perp = 13$–15 $g_\parallel = 2.035$, $^{N}A_\parallel = 17$	[35]
		$g_{iso} = 2.027$, $^{N}A_{iso} = 14.7$	[36]
$[Fe(CN)_5N(O)SR]^{3-}$	318 (1320) 526 (6000)	Diamagnetic	[19]
$[Fe(CN)_5SR]^{3-}$	700 (2700)		[11]
		$g_\perp = 2.126$, $g_\parallel = 2.086$ g_{iso} =2.086	This work
$[Fe(SR)_2(NO)_2]^{-}$	316, 363, 436 sh	$g_\perp = 2.0406$, $g_\parallel = 2.0120$ $g_{iso} = 2.0295$ $^{N}A_{iso} = 2.42$, $^{H}A_{iso} = 0.97$	This work
RSNO	230 (5100) 336 (840) 546 (13)	Diamagnetic	[37]
$RSNO^{\bullet -}$	~350	$g_\perp$= 2.0010, $^{N}A_\perp = 32$ $g_\parallel = 1.9299$, $^{N}A_\parallel = 7.2$	This work

substrate decayed within first 100 ns was transformed into the Fe(III) complex (Fig. 1a). Moreover, concentration of the $[Fe^{II}(CN)_5N(O)SR]^{3-}$ complex was almost completely regenerated within hundredths of a second, while concentration of the $[Fe^{III}(CN)_5SR]^{3-}$ product was kept constant (Fig. 1b).

In the photooxidation–substitution pathway, formation of the $[Fe^{III}(CN)_5SR]^{3-}$ complex and $RSNO^{\bullet -}$ radical was preceded by an increase and subsequent decay of weak transient absorption within the 300–380 nm, whose successive growth and fading were recorded within the first 15 ns (Figs. 1a, 2a and b). This may be assigned to the $[Fe^{III}(CN)_5\{N(O)SR\}^{\bullet}]^{3-}$ species and its time-resolved spectrum suggesting the decay by association/interchange mechanism (Scheme 1, path b) rather than by dissociation.

Although unequivocal assignment of the substitution mechanism was not possible, some additional arguments against the dissociation mechanism are coming from the concurrent photochemistry of nitroprusside (*vide infra*). Moreover, the tendency of the $[Fe(CN)_5N(O)SR]^{3-}$ and mercaptosuccinate anions to form ion pairs or aggregates [5,14,19] seems to support the association/interchange mechanism.

The second transient absorption which grows up within 15 ns, concurrently with that of the $[Fe^{III}(CN)_5SR]^{3-}$ complex, is characterised by λ_{max} at 350 nm and increase in absorption at $\lambda < 300$ nm (Figs. 1a and 2b). It decays with the half-life time of the order of microseconds ($\tau_{1/2} \sim 4\,\mu s$) and fits well to the $RSNO^{\bullet -}$ radical, whose generation was postulated also in other thiolate systems [29]. This attribution was supported by detection of a three-line ESR signal, assigned to the $RSNO^{\bullet -}$ radical (Fig. 3, Table 1). This signal, recorded in water–glycol glass at 77 K and decayed on annealing, is characterised by $g_\perp = 2.0010$, $g_\parallel = 1.9299$, $A_\perp(^{14}N) = 32$ G and $A_\parallel(^{14}N) = 7.2$ G. The parameters were calculated in orthorhombic approach although, as can be judged from the point symmetry of the $RSNO^{\bullet -}$ species, the actual symmetry may be lower (monoclinic). The high splitting constant suggests that the unpaired electron is localised mainly at the nitrogen atom and the distinct g-value shift from that of g_e can be explained by interaction of the unpaired electron with the sulphur atom [30–32].

2.2. Effect of nitroprusside

Owing to the equilibrium (Eq. (1)), nitroprusside is the inherent partner of the $[Fe(CN)_5N(O)SR]^{3-}$ complex in solution and, thus, its interference should be examined in detail. The main effects come from the very fast reactions in the equilibrium (Eq. (1)) and from the photochemical reactivity of the $[Fe(CN)_5NO]^{2-}$ complex.

The former effect, readily observed in nanosecond photolysis (Fig. 1), revealed an important aspect of the system: irradiation of the $[Fe(CN)_5N(O)SR]^{3-}$ component results in considerable acceleration of the reaction rate towards nitroprusside by contribution of the photodissociation mode (Scheme 1, path a), which unbalances the equilibrium (Eq. (1)) at delay times shorter than ~50 ms upon laser pulse (cf. Fig. 1b). This effect was used to estimate the second-order rate constant of the reaction between $[Fe(CN)_5NO]^{2-}$ and mercaptosuccinate (Eq. (1)). The value of $7.5 \times 10^3\,M^{-1}\,s^{-1}$ at 296 K was obtained, which is fairly consistent with the rate constant reported earlier by Johnson and Wilkins ($(3.2–3.6) \times 10^3\,M^{-1}\,s^{-1}$ at 298 K)

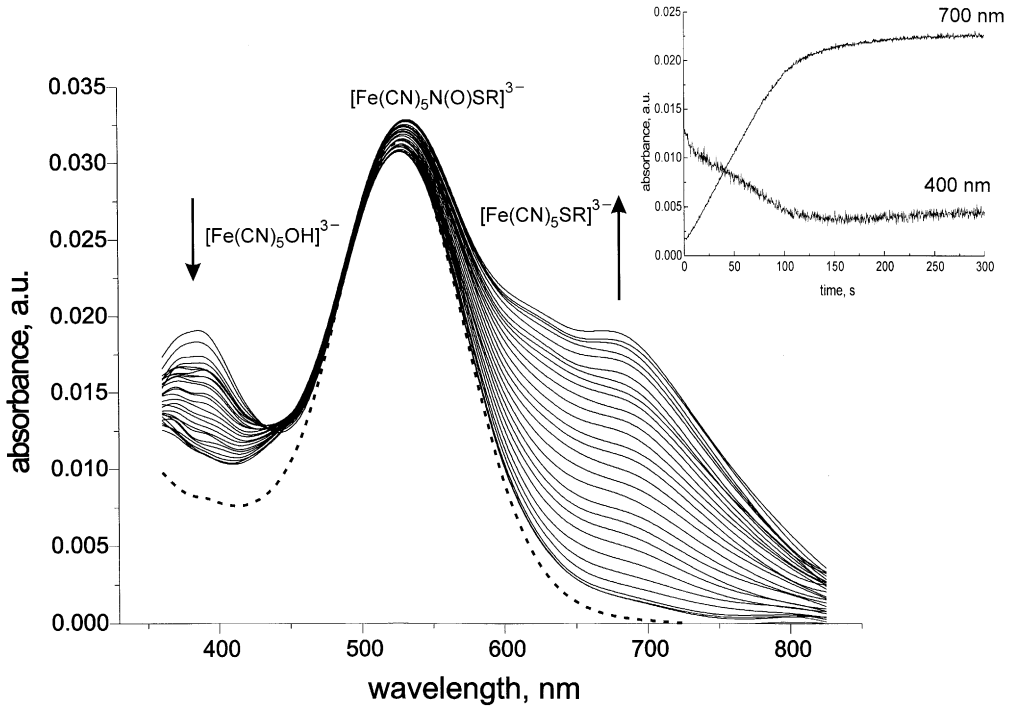

Fig. 4. Spectrum of the solution containing 4.9×10^{-6} M $[Fe(CN)_5N(O)SR]^{3-}$, 1.95×10^{-3} M $[Fe(CN)_5NO]^{2-}$ and 1.0×10^{-3} M RS^- (RS^- = mercaptosuccinate) before flash (dashed line) and spectral changes recorded every 5 s upon flashing with full light of the xenon lamp (solid lines); insert shows the kinetic traces at wavelengths characteristic of the $[Fe(CN)_5SR]^{3-}$ (700 nm) and $[Fe(CN)_5OH]^{3-}$ (400 nm) complexes.

[13], although completely different methods were used and the experimental conditions differed in some details. The consequences of the drastic change in reaction rate were also observed under continuous irradiation within the spectral range of the $[Fe(CN)_5N(O)SR]^{3-}$ absorption. Then the photochemically induced shift of the equilibrium (Eq. (1)) to the left was observed, and the equilibrium constant in photostationary state (K_{ph}) was significantly lower than the constant in the dark (K_d).

Photochemical reactivity of nitroprusside can really interfere with that of $[Fe(CN)_5N(O)SR]^{3-}$ only at irradiation wavelengths shorter than ~400 nm, i.e. when NP absorption starts to be detectable (cf. Table 1) and its quantum yield exceeds that of the thiolate derivative [11]. This is the reason why laser photolysis at $\lambda = 355$ nm leads to generation not only of $[Fe^{III}(CN)_5SR]^{3-}$, but also of the $[Fe^{III}(CN)_5OH]^{3-}$ complex, which is the known photo oxidation product of nitroprusside in alkaline medium [21–27]. Absorption characteristic of the hydroxo complex (with a maximum at ~400 nm) is observed up to delay times of the order of seconds. At still longer delay times, however, the $[Fe(CN)_5SR]^{3-}$ concentration increases at the cost of the hydroxo complex, due to the substitution reaction

$$[Fe^{III}(CN)_5OH]^{3-} + RS^- \rightarrow [Fe^{III}(CN)_5SR]^{3-} + OH^- \quad (6)$$

which is a relatively slow process. Its estimated second-order rate constant at 296 K is roughly $k \approx 4.5\,M^{-1}\,s^{-1}$. The substitution reaction (Eq. (6)) is illustrated by the spectral changes recorded within seconds upon flash photolysis by full xenon light, which excites mostly the $[Fe(CN)_5NO]^{2-}$ complex and thereby the initial spectra of the flashed solution are characteristic mainly of the NP photoproduct (Fig. 4).

The substitution of the OH^- by mercaptosuccinate (Eq. (6)) was so verified by monitoring an increase in the ESR signal at $g_{iso} = 2.086$ characteristic of the $[Fe(CN)_5SR]^{3-}$, but not of the $[Fe^{III}(CN)_5OH]^{3-}$ complex.

In conclusion, photochemical conversion of $[Fe(CN)_5NO]^{2-}$ into $[Fe(CN)_5OH]^{3-}$, instead of $[Fe(CN)_5SR]^{3-}$, even in the presence of an excess of mercaptosuccinate (e.g. in 5:1 molar ratio), seems to exclude the $[Fe(CN)_5]^{2-}$ precursor of these products. Thus, the dissociation mechanism of the photooxidation–substitution is in our opinion less probable.

2.3. Secondary processes

Amongst the primary products of the $[Fe(CN)_5N(O)SR]^{3-}$ photooxidation–substitution (Scheme 1), the $[Fe^{III}(CN)_5SR]^{3-}$ complex is relatively stable, whereas the $RSNO^{\bullet -}$ radical is highly reactive [38,39]. Its decay, observed within ~100 ms, is accompanied by hypsochromic shift of the 350 nm band to ~330 nm with simultaneous increase in absorption (cf. Figs. 1b and 2c). The spectral region, however, is not specific (cf. Fig. 6b) and, therefore, the fate of the $RSNO^{\bullet -}$ radical was followed mostly by ESR method.

Table 2
ESR characteristics of different $[Fe^{-I}L_2(NO)_2]^{n-}$ complexes[a]

Ligands	77 K		Room temperature			Reference
	$g_\perp$	$g_\parallel$	g_{iso}	A_{iso} (^{14}N)	A_{iso} (^{1}H)	
Mercaptosuccinate	2.0406	2.0120	2.0295	2.42	0.97	This work
Glutathione	2.04	2.01	–	–	–	[40]
Cysteine	2.04	2.01	–	–	–	[41]
Cysteine	2.039	2.013	2.028	1.2	1.2	[42]
$(CH_3)_2CHS^-$	–	–	2.028	2.5	0.5	[42]
$(CH_3)_2CHS^-$	–	–	2.027	2.5	1.3	[43]
$CH_3CH_2CH(CH_3)S^-$	–	–	2.028	2.5	0.5	[42]
HS^-	–	–	2.028	2.7	0.5	[43]
CH_3S^-	–	–	2.028	2.1	2.1	[43]
$(CH_3)_3CS^-$	–	–	2.027	2.7	–	[43]
$C_6H_5CH_2S^-$	–	–	2.027	2.4	1.4	[43]
$CH_3CH_2CH_2S^-$	–	–	2.028	1.2	1.2	[42]
$CH_3CH_2CH_2CH_2S^-$	–	–	2.028	1.2	1.2	[42]
$CH_3(CH_2)_{10}CH_2S^-$	–	–	2.028	1.2	1.2	[42]
$HOCH_2CH_2S^-$	–	–	2.028	1.2	1.2	[42]
Homocysteine	–	–	2.028	1.2	1.2	[42]
2-Mercaptobenzimidazole-*S*	2.039	2.013	2.028	2.5	–	[42]
2-Mercaptobenzimidazole-*N*	2.040	2.012	2.029	2.5	–	[42]
2-Mercaptobenzoxazole-*S*	2.040	2.013	2.029	~2	–	[42]
1,2,3-Benzotriazole	–	–	2.027	2.5	–	[42]
DMF	–	–	2.033	2.4	4.0	[43]
DMF, $(CH_3)_2CHS^-$	–	–	2.027	2.6	1.3, 4.6	[43]
DMA	–	–	2.033	2.5	–	[43]
DMA, $(CH_3)_2CHS^-$	–	–	2.027	2.5	1.3	[43]
Pyridine	–	–	2.031	2.2, 4.5	–	[43]
DMSO, CH_3S^-	–	–	2.032	6.0	3.2	[43]
2,6-Dimethylpyridine	–	–	2.031	2.3, 4.6	–	[43]
Quinoline	–	–	2.032	2.2, 4.4	–	[43]
$(CH_3CH_2)_2NH$, CH_3S^-	–	–	2.030	4.0	2.0	[43]
Pyrrolidine, CH_3S^-	–	–	2.029	4.2	2.0	[43]
Piperidine, CH_3S^-	–	–	2.029	4.2	2.1	[43]
Pyrrolidine, $C_6H_5CH_2S^-$	–	–	2.029	4.2	2.0	[43]

[a] Abbreviations: DMF, dimethylformamide; DMA, dimethylacetamide; DMSO, dimethylsulphoxide.

The spectra shown in Fig. 3 demonstrate that decay of the signal of the $RSNO^{\bullet-}$ radical (see Table 1) is accompanied by an increase in another signal with $g_\perp = 2.0406$ and $g_\parallel = 2.012$ at 77 K. The registration of new species at room temperature allowed us to determine not only $g_{iso} = 2.0295$, but also the hyperfine splittings $A_{iso}(^{14}N) = 2.42$ G, and $A_{iso}(^{1}H) = 0.97$ G. The $g_\parallel < g_\perp$ indicates that the ground state is largely confined to d_{z^2} orbital. The spectrum is characteristic of the dinitrosyl tetrahedral complexes, containing formally the Fe(–I) centre, $[FeL_2(NO)_2]^-$ [40–43]. The ESR signals of these compounds are only slightly dependent on the thiol structure and can be treated as finger print of this class of the complexes (Table 2).

The dinitrosyldithiolatoferrate(–I) complexes have been known since long as produced thermally from nitroprusside at extremely high thiolate excess and at elevated temperature [44]. Under conditions applied in this work $[Fe(SR)_2(NO)_2]^-$ was formed only in consequence of the photochemical reaction of the $[Fe(CN)_5N(O)SR]^{3-}$ complex. In all studied cases, even at very low thiolate concentration, the dinitrosyl complex, $[Fe(SR)_2(NO)_2]^-$, appeared to be the main paramagnetic species containing reduced Fe centre. Beside this dominant product, however, a minor amount of $[Fe^{I}(CN)_5NO]^{3-}$ (Table 1) was also detected. The formation of $[Fe(SR)_2(NO)_2]^-$, but not of $[Fe^{I}(CN)_5NO]^{3-}$, was found to be strongly affected by the thiolate concentration: the Fe(–I)/Fe(I) ratio was never <2; whereas even at moderate RS^- excess this ratio increases easily by two-orders of magnitude (cf. Fig. 5).

Thus, the oxidative decay of the $RSNO^{\bullet-}$ radicals is responsible for the reduction of the iron complexes. As nitrosyl and dinitrosyl species are here produced, both nitroprusside and its thiolate derivative can be the main targets of the $RSNO^{\bullet-}$ attack. As in other cases [45], the Fe(I) complex is expected to be produced from NP by an electron transfer (Eq. (7))

$$[Fe^{II}(CN)_5NO]^{2-} + RSNO^{\bullet-} \rightarrow [Fe^{I}(CN)_5NO]^{3-} + RSNO \quad (7)$$

which is thermodynamically allowed due to the favourable redox potentials of the reagents: $E_{[Fe(CN)_5NO]^{2-}/[Fe(CN)_5NO]^{3-}}$

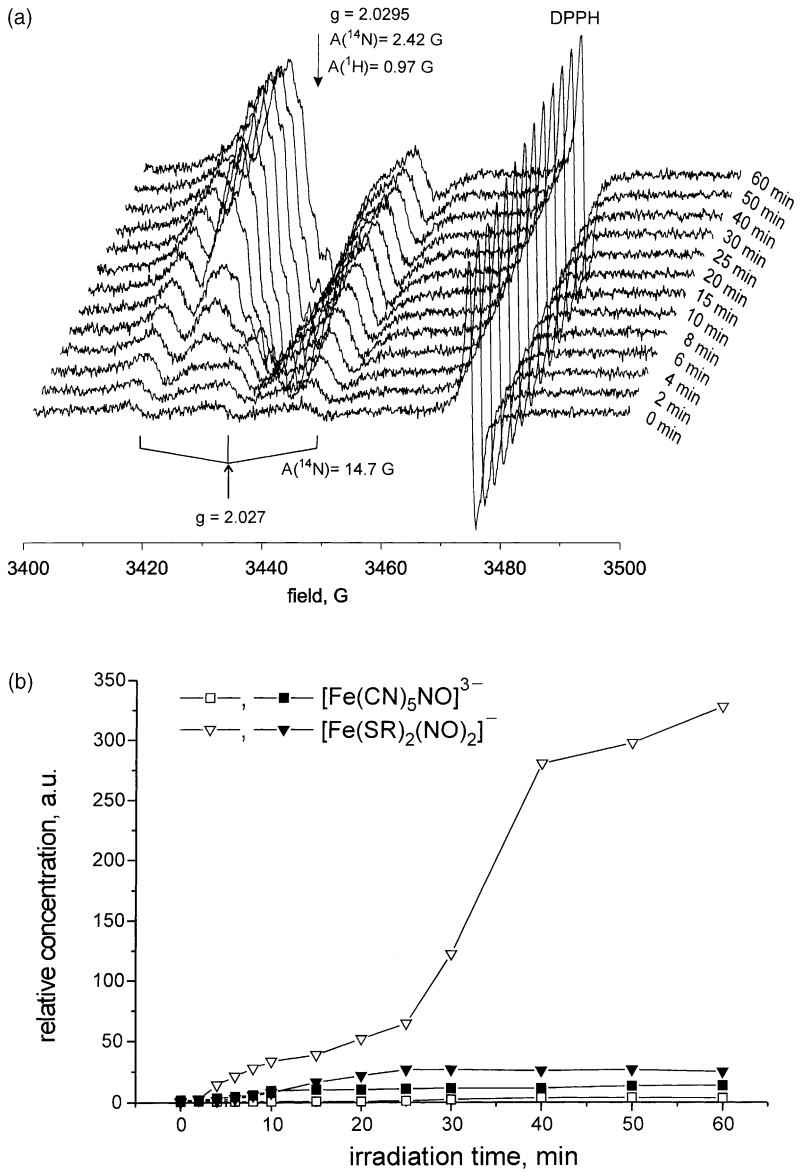

Fig. 5. (a) Time-resolved ESR spectra recorded during continuous 545 nm photolysis of $[Fe(CN)_5N(O)SR]^{3-}$ generated from 0.05 M $[Fe(CN)_5NO]^{2-}$ in the presence of 3.33×10^{-3} M RS^- (RS^- = mercaptosuccinate); (b) time dependence of $[Fe(SR)_2(NO)_2]^-$ and $[Fe^{I}(CN)_5NO]^{3-}$ concentrations as derived from the ESR analysis for the nitroprusside-to-thiolate initial ratio 1:5 (empty marks) and 15:1 (black marks).

$= -0.3$ V versus Ag/AgCl and $E_{RSNO/RSNO^{\bullet -}} = -1.0$ V versus Ag/AgCl (reported by [39] and [45], respectively, and confirmed in this study).

The Fe(–I) complex could be formed as a result of interaction between the $RSNO^{\bullet -}$ radical and one of the CN^- ligands in nitroprusside or its thiolate derivative. It is difficult to assess the role of the two above targets, but there are some arguments advocating the $[Fe(CN)_5N(O)SR]^{3-}$ complex. Firstly, the reaction is affected by a large RS^- excess that shifts the equilibrium (Eq. (1)), decreasing nitroprusside and increasing the $[Fe(CN)_5N(O)SR]^{3-}$ concentrations. Secondly, if the nucleophilic attack of the coordinated CN^- is responsible for the Fe(–I) production, the more favoured target would be the complex with weaker Fe–NO bond (i.e. the thiolate derivative).

In oxygenated solutions, the $RSNO^{\bullet -}$ radical decays as well in reaction with oxygen [38] (Eq. (8)).

$$RSNO^{\bullet -} + O_2 \rightarrow RSNO + O_2^{\bullet -} \quad (8)$$

Unfortunately, in such a case another active species ($O_2^{\bullet -}$) is produced that additionally complicates the already complex system. Finally, another conceivable pathway of the $RSNO^{\bullet -}$ decay is also its dissociation [39].

$$RSNO^{\bullet -} \rightarrow RS^- + NO^{\bullet} \quad (9)$$

Besides the $RSNO^{\bullet -}$ radicals, also the products containing reduced iron undergo oxidation by O_2 leading to formation of Fe(II) complexes as stable products.

2.4. Product analysis

Any practical application of a system needs the recognition of its stable products, or products stable enough to be used in required procedures. In the studied system the compounds are: RSNO, $[Fe^{III}(CN)_5SR]^{3-}$, $[Fe(SR)_2(NO)_2]^-$, and $[Fe^{I}(CN)_5NO]^{3-}$. At least two of them, $[Fe(SR)_2(NO)_2]^-$ and RSNO, are of medical importance. Unfortunately, using UV/VIS spectroscopy, only the $[Fe(CN)_5N(O)SR]^{3-}$ substrate decay (decrease in absorption at 526 nm) and formation of the $[Fe(CN)_5SR]^{3-}$ product (increase in absorption at 700 nm) can be followed directly. The results are exemplified in Fig. 6a.

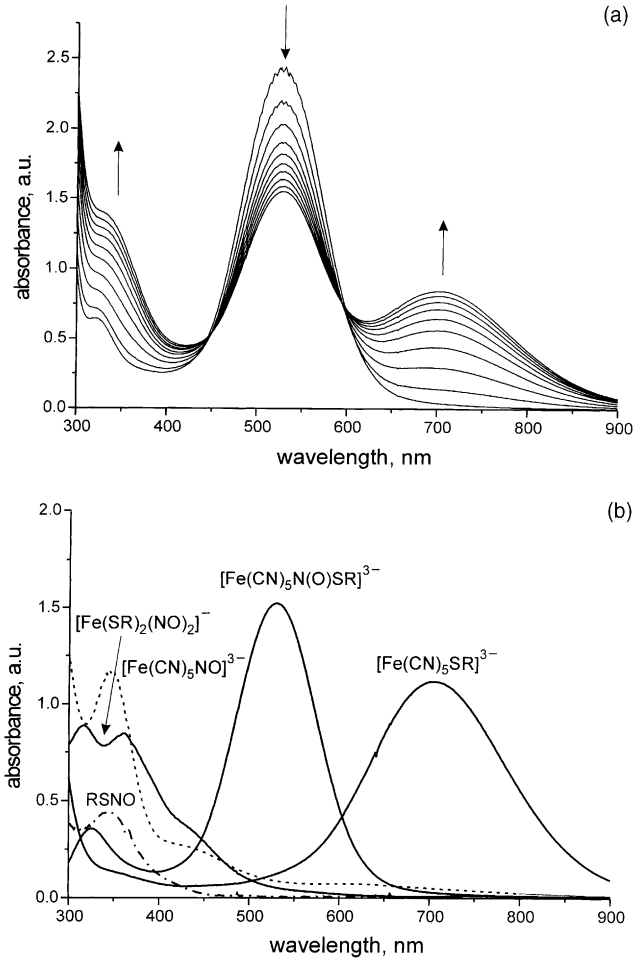

Fig. 6. (a) Spectral changes recorded during irradiation (λ_{irr} 578 nm) of aerated solution of 3.9×10^{-4} M $[Fe(CN)_5N(O)SR]^{3-}$ in the presence of 2.1×10^{-3} M $[Fe(CN)_5NO]^{2-}$, and 0.0125 M RS^- (RS^- = mercaptosuccinate) at pH 10; (b) spectra of reagents and relatively stable products calculated by means of SPEXFA programme using experimental data shown in (a).

Concentrations of other components could be evaluated only indirectly: the amount of $[Fe(CN)_5NO]^{2-}$ was estimated from the equilibrium constant (Eq. (1)); whereas the sum of the minor products containing Fe(II), Fe(I) and Fe(–I) complexes was assessed basing on their similar absorption within 450–300 nm (together with the parent $[Fe(CN)_5N(O)SR]^{3-}$). To solve the problem, the spectral isolation factor analysis (SPEXFA) was used to separate the product spectra from the experimental curves. The results of the numerical analysis, compared with the genuine spectra of the components, were consistent with the expected composition of irradiated solutions (Fig. 6b). The spectrophotometric measurements were completed by analytical detection (using Saville's method [46]) of the products containing weakly bonded NO, i.e. compounds being potential NO-donors, such as *S*- nitrosomercaptosuccinate or $[Fe(SR)_2(NO)_2]^-$ (Fig. 7).

The results of the continuous photolysis, although only approximate, indicated that:

1. Concentration of the photochemically produced $[Fe^{I}(CN)_5NO]^{3-}$ depends strongly on the presence of oxygen; only in deaerated solutions the Fe(I) complex is generated in significant amounts. This points to a substantial contribution of the nitroprusside in scavenging the $RSNO^{\bullet -}$ radicals (Eq. (7)) in the absence of oxygen. In the aerated system, O_2 is obviously among the principal radical scavengers (Eq. (8)).
2. Photochemistry of $[Fe(CN)_5N(O)SR]^{3-}$ produces NO-donors in amount not lower than that of $[Fe^{III}(CN)_5SR]^{3-}$ (cf. Fig. 7). This means that nitrosation capacity of the system acquired in the photooxidation–substitution reaction (Scheme 1, path b) is not significantly reduced

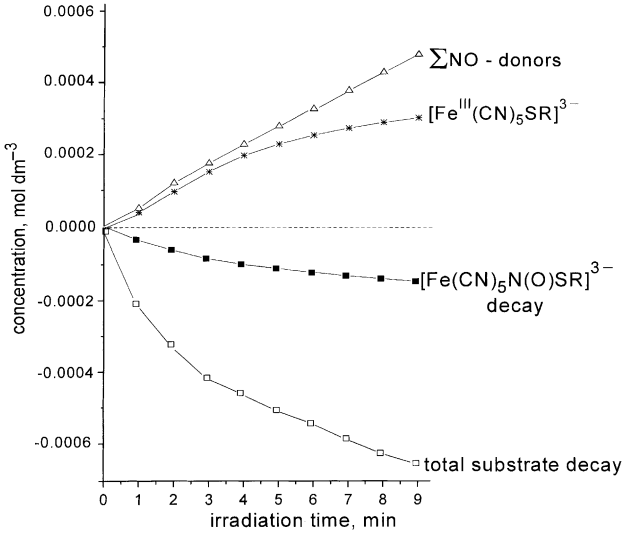

Fig. 7. Time dependence of substrate decay ($[Fe(CN)_5N(O)SR]^{3-}$ and sum of $[Fe(CN)_5N(O)SR]^{3-}$ and $[Fe(CN)_5NO]^{2-}$) compared with product formation ($[Fe(CN)_5SR]^{3-}$ and sum of NO-donors); experimental conditions as in Fig. 6.

as a result of the secondary processes. The contribution from dissociation of the $RSNO^{\bullet-}$ radical (Eq. (9)) can thus be neglected.

3. Photoproduction of the $[Fe(CN)_5SR]^{3-}$ complex is accompanied by its slow thermal decomposition ($\tau_{1/2}$ = 650 s [11]), which reduces its actual concentration especially at longer irradiation times (Fig. 7). When the actual concentrations are corrected for the thermal decomposition, the c versus t_{irr} plot for $[Fe(CN)_5SR]^{3-}$ nearly overlaps that for the total NO-donors. The $[Fe(CN)_5SR]^{3-}$ concentration in photolyte is always higher than the decrease in concentration of the parent $[Fe(CN)_5N(O)SR]^{3-}$ complex, which means that not only $[Fe(CN)_5N(O)SR]^{3-}$, but also nitroprusside are consumed in the photochemical process.
4. Analysis of the substrate decay, i.e. both $[Fe(CN)_5NO]^{2-}$ and $[Fe(CN)_5N(O)SR]^{3-}$, leads to a conclusion that the decay is always at least two times larger than the increase in $[Fe^{III}(CN)_5SR]^{3-}$ concentration (e.g. Fig. 7). This indicates that the quantum yield values of the $[Fe^{III}(CN)_5SR]^{3-}$ production reported earlier [11] do not represent the total yields of the substrate decay, which are actually more than two times higher.
5. Moreover, it is the $[Fe(CN)_5NO]^{2-}$ complex, not the $[Fe(CN)_5N(O)SR]^{3-}$, that is mostly consumed in the photochemical reaction, even when the irradiating light is not absorbed directly by nitroprusside (e.g. 578 nm). In different experiments, the contribution of nitroprusside to the total substrate loss amounted to 80–85% (Fig. 7). The value was higher in deaerated photolytes, consistent with nitroprusside contribution to scavenging the $RSNO^{\bullet-}$ radicals (cf. point (1)).

The results indicate that the studied reaction is in reality an indirect photooxidation–substitution of $[Fe(CN)_5NO]^{2-}$, catalysed by the mercaptosuccinate anion. The reaction may be defined as photoassisted reaction in which nitroprusside may be treated as a substrate, mercaptosuccinate anion as a photoactivator, whereas the $[Fe(CN)_5N(O)SR]^{3-}$ complex plays a role of the substrate–activator adduct, which undergoes the photochemical reaction.

3. Conclusions

All the results testify that the $[Fe(CN)_5N(O)SR]^{3-}$–$[Fe(CN)_5NO]^{2-}$– thiolate system is potentially suitable for photomedical applications. For RS^- = mercaptosuccinate, the nitrosothiol complex is thermally stable and absorbs strongly near the phototherapeutic window. Irradiation of the complex with the low energy light causes generation of moderately reactive nitrosation agents, such as *S*-nitrosomercaptosuccinate and $[Fe(SR)_2(NO)_2]^-$, which are known as medically relevant compounds. In addition, the nitrosation capacity of the system does not decay in course of the secondary reactions.

Due to the fast reactions in equilibrium between nitroprusside and its thiolate derivative (Eq. (1)), the process is photocatalytic in character. This means that the nitrosation agents are produced at the expense of nitroprusside although the $[Fe(CN)_5N(O)SR]^{3-}$ complex absorbs light and undergoes the photooxidation–substitution reaction (Scheme 1, path b). Moreover, because there is a variety of nucleophiles available, which can form similar substrate–activator adducts equilibrated with nitroprusside [12,14,18,19,47,48], the photoassistance may be responsible as well for photochemical behaviour of $[Fe(CN)_5NO]^{2-}$ in many other systems.

Furthermore, the studied system is highly manipulatable and allows changing its reactivity by modification of the reaction conditions. The equilibrium between nitroprusside and its thiolato derivative (Eq. (1)) is sensitive to many parameters, such as temperature, pressure [49,50], pH, ionic strength, concentration and nature of cations [5,14,19,49,50], and additionally to the intensity and wavelengths of irradiating light. Thus, change in the reagent ratio, irradiation conditions, medium viscosity, pH, concentration of oxygen, ionic strength and even nature of the cations can modulate the reaction course, quantum yield and ratio of the produced compounds.

4. Experimental

The $[Fe(CN)_5N(O)SR]^{3-}$ complex was generated in situ from sodium nitroprusside and mercaptosuccinic acid [19]. All other chemicals were of analytical purity (Aldrich). Carbonate–borate buffer of pH 10 was prepared from triply distilled water and used in all the experiments.

ESR spectra were recorded at 77 K on Bruker ELEXYS 500 spectrometer operating at the X band with 100 kHz modulation. Glass containing 0.1 M K_2CO_3 and 1,3-propanediol (1:1 v/v) was used as a reaction medium. Room temperature ESR measurements were performed on Bruker EMS spectrometer in flat quartz cells with DPPH as internal standard. ESR spectra were analysed using PEST Winsim 0.96 [52] and SIM14S [53] software. UV/VIS spectra were recorded on Shimadzu UV/VIS 2100, Hewlett-Packard HP 8463 and Ocean Optics SD-1000 spectrophotometers in 1 cm quartz cells. Factor analysis was performed using Target 96M software (MATLAB version) [54]. A high-pressure mercury lamp (HBO 200) equipped with LPS 250 power supply (Photon Technology International) was used as a light source; chosen wavelengths were selected using interference filters. Nanosecond photolysis was performed using laser spectrometer LKS 50 (Applied Photophysics) equipped with Nd-YAG laser Surelite Sl I-10 (Continuum). Microsecond flash photolysis apparatus was home made with a xenon lamp [49,51]. Electrochemical measurements were performed on BAS CV 50W electrochemical analyser (Bioanalytical Systems) with glassy carbon working electrode, and Ag/AgCl reference electrode FLEXREF (World Precision Instruments). *S*-nitrosothiol and other NO-donors

were determined quantitatively using Saville's method [46]. Before the analysis samples were acidified and oxygenated to transform $[Fe(CN)_5N(O)SR]^{3-}$ and $[Fe(CN)_5NO]^{3-}$ into nitroprusside.

Acknowledgements

We gratefully acknowledge financial support from KBN, grants nos. PB 0341/T09/98/15 and C-050. Authors thank Professor Orazio Traverso for helpful discussions, Ms. Ewa Bidzińska for her assistance in low temperature ESR measurements and Dr. Andrzej Turek for his help in numerical analysis of UV/VIS spectra.

References

[1] P.C. Ford, J. Bourassa, K. Miranda, B. Lee, I. Lorkovic, S. Boggs, S. Kudo, L. Laverman, Coord. Chem. Rev. 171 (1998) 185.
[2] G. Stochel, A. Wanat, E. Kuliś, Z. Stasicka, Coord. Chem. Rev. 171 (1998) 203.
[3] J. Bourassa, W. De Graff, S. Kudo, D.A. Wink, J.B. Mitchell, P.C. Ford, J. Am. Chem. Soc. 119 (1997) 2853.
[4] J. Bourassa, B. Lee, S. Bernard, J. Schoonover, P.C. Ford, Inorg. Chem. 38 (1998) 2947.
[5] K. Szaciłowski, W. Macyk, G. Stochel, Z. Stasicka, S. Sostero, O. Traverso, Coord. Chem. Rev. 208 (2000) 277.
[6] J.L. Bourassa, P.C. Ford, Coord. Chem. Rev. 200–202 (2000) 887.
[7] M.A. DeLeo, P.C. Ford, J. Am. Chem. Soc. 121 (1999) 1980.
[8] M.A. DeLeo, P.C. Ford, Coord. Chem. Rev. 208 (2000) 47.
[9] D.R. Adams, M. Brochwicz-Lewinski, A.R. Butler, Progr. Chem. Org. Nat. Prod. 76 (1999) 1.
[10] D.J. Sexton, A. Muruganandam, D. McKenney, B. Mutus, Photochem. Photobiol. 59 (1994) 463.
[11] K. Szaciłowski, J. Oszajca, G. Stochel, Z. Stasicka, J. Chem. Soc., Dalton Trans. 2353 (1999).
[12] A.R. Butler, C. Glidewell, Chem. Soc. Rev. 16 (1987) 361.
[13] M.D. Johnson, R.G. Wilkins, Inorg. Chem. 23 (1984) 231.
[14] R. Leeuwenkamp, C.H. Vermaat, C.H. Plug, A. Bult, Pharm. Weekbl. Sci. 6 (1984) 195.
[15] K. Antay, J. Banyai, M. Beck, J. Chem. Soc., Dalton Trans. 1191 (1985).
[16] A.R. Butler, A.M. Calsy-Harrison, C. Glidewell, I.L. Johnson, J. Regliński, W.B. Smith, Inorg. Chim. Acta 151 (1988) 281.
[17] A.R. Butler, A.M. Calsy-Harrison, C. Glidewell, P.E. Sorensen, Polyhedron 7 (1988) 1197.
[18] A.R. Butler, A.M. Calsy, I.L. Johnson, Polyhedron 9 (1990) 913.
[19] K. Szaciłowski, G. Stochel, Z. Stasicka, H. Kirsch, New. J. Chem. 21 (1997) 893.
[20] P.J. Morando, E.B. Borghi, L.M. de Schteingart, M.A. Blesa, J. Chem. Soc., Dalton Trans. 435 (1981).
[21] G. Stochel, Z. Stasicka, Polyhedron 4 (1985) 1887.
[22] G. Stochel, R. van Eldik, Z. Stasicka, Inorg. Chem. 25 (1986) 3663.
[23] Z. Stasicka, E. Wasielewska, Coord. Chem. Rev. 159 (1997) 271.
[24] S. Kudo, J.L. Bourassa, S.E. Boggs, Y. Sato, P.C. Ford, Anal. Biochem. 247 (1997) 193.
[25] S.K. Wolfe, J.H. Swinehart, Inorg. Chem. 14 (1975) 1049.
[26] K.S. Sidhu, W.R. Bansal, Ms. Sumanjit, J. Photochem. Photobiol. A: Chem. 65 (1992) 355.
[27] M.G. De Oliveira, J. Langley, A.J. Rest, J. Chem. Soc., Dalton Trans. 2013 (1995).
[28] B.A. Goodman, J.B. Raynor, Adv. Inorg. Chem. Radiochem. 13 (1970) 136.
[29] N. Arulsalmy, D.S. Bohle, J.A. Butt, G.J. Irvine, P.A. Jordan, E. Sagan, J. Am. Chem. Soc. 121 (1999) 7115.
[30] K. Akasako, J. Chem. Phys. 43 (1965) 1182.
[31] Y. Kurita, W. Gordy, J. Chem. Phys. 34 (1961) 282.
[32] W.A. Waters, J. Chem. Soc., Chem. Commun. 741 (1978).
[33] E. Wasielewska, Z. Stasicka, J. Inf. Rec. Mater. 17 (1989) 441.
[34] R.P. Cheney, M.G. Simic, M.Z. Hoffman, I.A. Taub, K.D. Asmus, Inorg. Chem. 16 (1977) 2187.
[35] M.C.R. Symons, J.G. Wilkinson, D.X. West, J. Chem. Soc., Dalton Trans. 2041 (1982).
[36] J.D.W. Van Voorst, P. Hemmerich, J. Chem. Phys. 45 (1966) 3914.
[37] K. Szacłowski, Z. Stasicka, Prog. React. Kin. Mech. 25 (2000) 1.
[38] A.J. Gow, D.G. Buerk, H. Ischiropoulos, J. Biol. Chem. 272 (1997) 2841.
[39] Y. Hou, J. Wang, F. Arias, L. Echegoyen, P.G. Wang, Bioorg. Med. Chem. Lett. 8 (1998) 3065.
[40] M. Boese, M.A. Keese, K. Becker, R. Busse, A. Mülsch, J. Biol. Chem. 35 (1997) 21767.
[41] F.C.A. Wiegant, I.Y. Malyshev, A.L. Kleschyov, E. van Faassen, A.F. Vanin, FEBS Lett. 455 (1999) 179.
[42] B. Jeżowska-Trzebiatowska, A. Jezierski, J. Mol. Struct. 19 (1973) 635.
[43] A.R. Butler, C. Glidewell, M.H. Li, Adv. Inorg. Chem. 32 (1988) 335.
[44] N.S. Garifyanov, S.A. Luchkina, Dokl. Akad. Nauk SSSR 189 (1969) 219.
[45] H.M. Carapuca, J.E.J. Simao, A.G. Fogg, Analyst 121 (1996) 1801.
[46] M. Marzinzig, A.K. Nussler, J. Stadler, E. Marzinzig, W. Barthlen, N.C. Nussler, H.G. Beger, S.M. Morris Jr., U.B. Brückner, Nitric Oxide 1 (1997) 177.
[47] F. Bottomley, Acc. Chem. Res. 11 (1978) 158.
[48] J.A. McCleverty, Chem. Rev. 79 (1979) 53.
[49] K. Szaciłowski, Ph.D. Dissertation, Jagiellonian University, Kraków, Poland, 2000.
[50] K. Szaciłowski, A. Barbieri, A. Wanat, S. Sostero, O. Traverso, G. Stochel, Z. Stasicka, in preparation.
[51] T. Jarzynowski, T. Senkowski, Z. Stasicka, Pol. J. Chem. 55 (1981) 3.
[52] D. Duling, Public EPR Software Tools, 1996, available at: http://alfred.niehs.nih.gov/LMB.
[53] G.P. Lozos, B.M. Hoffman, C.G. Frank, QCHPE.
[54] M.M. Darj, E.R. Malinowski, Anal. Chem. 68 (1996) 1593.